

Computer Assisted Planning, Simulation and Navigation of Periacetabular Osteotomy

Li Liu¹, Timo M. Ecker², Klaus-A. Siebenrock², and Guoyan Zheng¹(✉)

¹ Institute for Surgical Technology and Biomechanics,
University of Bern, Bern, Switzerland
{li.liu, guoyan.zheng}@istb.unibe.ch

² Department of Orthopedic Surgery, Inselspital,
University of Bern, Bern, Switzerland

Abstract. Periacetabular osteotomy (PAO) is an effective approach for surgical treatment of hip dysplasia in young adults. However, achieving an optimal acetabular reorientation during PAO is the most critical and challenging step. Routinely, the correct positioning of the acetabular fragment largely depends on the surgeons experience and is done under fluoroscopy to provide the surgeon with continuous live x-ray guidance. To address these challenges, we developed a computer assisted system. Our system starts with a fully automatic detection of the acetabular rim, which allows for quantifying the acetabular 3D morphology with parameters such as acetabular orientation, femoral head Extrusion Index (EI), Lateral Center Edge (LCE) angle, total and regional femoral head coverage (FHC) ratio for computer assisted diagnosis, planning and simulation of PAO. Intra-operative navigation is used to implement the pre-operative plan. Two validation studies were conducted on four sawbone models to evaluate the efficacy of the system intra-operatively and post-operatively. By comparing the pre-operatively planned situation with the intra-operatively achieved situation, average errors of $0.6^\circ \pm 0.3^\circ$, $0.3^\circ \pm 0.2^\circ$ and $1.1^\circ \pm 1.1^\circ$ were found respectively along three motion directions (Flexion/Extension, Abduction/Adduction and External Rotation/Internal Rotation). In addition, by comparing the pre-operatively planned situation with the post-operative results, average errors of $0.9^\circ \pm 0.3^\circ$ and $0.9^\circ \pm 0.7^\circ$ were found for inclination and anteversion, respectively.

1 Introduction

Developmental dysplasia of the hip joint is a prearthrotic deformity resulting in osteoarthritis at a very young age. Periacetabular Osteotomy (PAO) is an effective approach for surgical treatment of painful dysplasia of the hip in younger patients [1]. The aim of PAO is to increase acetabular coverage of the femoral head and to reduce contact pressures by realigning the hip joint [2,3]. However, insufficient reorientation leads to continued instability while excessive reorientation correction would result in femoroacetabular impingement (FAI) [4,5]. Therefore, a main important factor for clinical outcome and long-term success of PAO

is to achieve an optimal acetabular reorientation [6]. The application of computer assisted planning and navigation in PAO opens such an opportunity by showing its potential to improve surgical outcomes in PAO. Before the PAO-specific navigation system was introduced, some commercially available navigation systems were modified and adapted for PAO clinical trials. Abraham et al. [7] presented an experimental cadaver study in order to investigate the utility of pre-operative 3D osteotomy planning and intra-operative acetabular repositioning in the navigated PAO surgery. Hsieh et al. [8] assessed the efficacy of the navigated PAO procedure in 36 clinical cases using a modified version of commercially available navigation program for THA (VectorVision, BrainLab Inc., Westchester, IL). Seminal work has been done by Langlotz et al. [9], who developed the first generation of CT-based customized navigation system for PAO and applied it to 14 clinical cases. However, this system only focuses on navigated osteotomy procedure while reorientation procedure is lack of standard morphological parameters feedback. More recently, Murphy et al. [10] developed a computer assisted Biomechanical Guidance System (BGS) for performing PAO. The system combines geometric and biomechanical feedback with intra-operative tracking to guide the surgeon through the PAO procedure. In this paper, we developed and validated a novel computer assisted diagnosis, planning, simulation and navigation system for PAO. It is hypothesized that the pre-operative plan done with our system can be achieved by the navigated PAO procedure with a reasonable accuracy.

2 Materials and Methods

2.1 System Workflow

The computer assisted diagnosis, planning, simulation and navigation system for PAO consists of three modules as shown in Fig. 1.

- **Model generation module.** 3D surface models of the femur and the pelvis are generated by fully automatic segmentation of the pre-operatively acquired CT data [11].
- **Computer assisted diagnosis, planning and simulation module.** The aim of this module is first to quantify the 3D hip joint morphology for a computer assisted diagnosis of hip dysplasia, and then to plan and simulate the reorientation procedure using the surface models generated from the model generation module. It starts with a fully automatic detection of the acetabular rim, which allows for computing important information quantifying the acetabular morphology such as femoral head coverage (FHC), femoral head extrusion index (EI), lateral centre edge (LCE) angle, version and inclination. This module then provides a graphical user interface allowing the surgeon to conduct a virtual osteotomy and to further reorient the acetabular fragment until an optimal realignment is achieved.
- **Intra-operative navigation module.** Based on an optical tracking technique, this module aims for providing intra-operative visual feedback during acetabular fragment osteotomy and reorientation until the pre-operatively planned orientation is achieved.

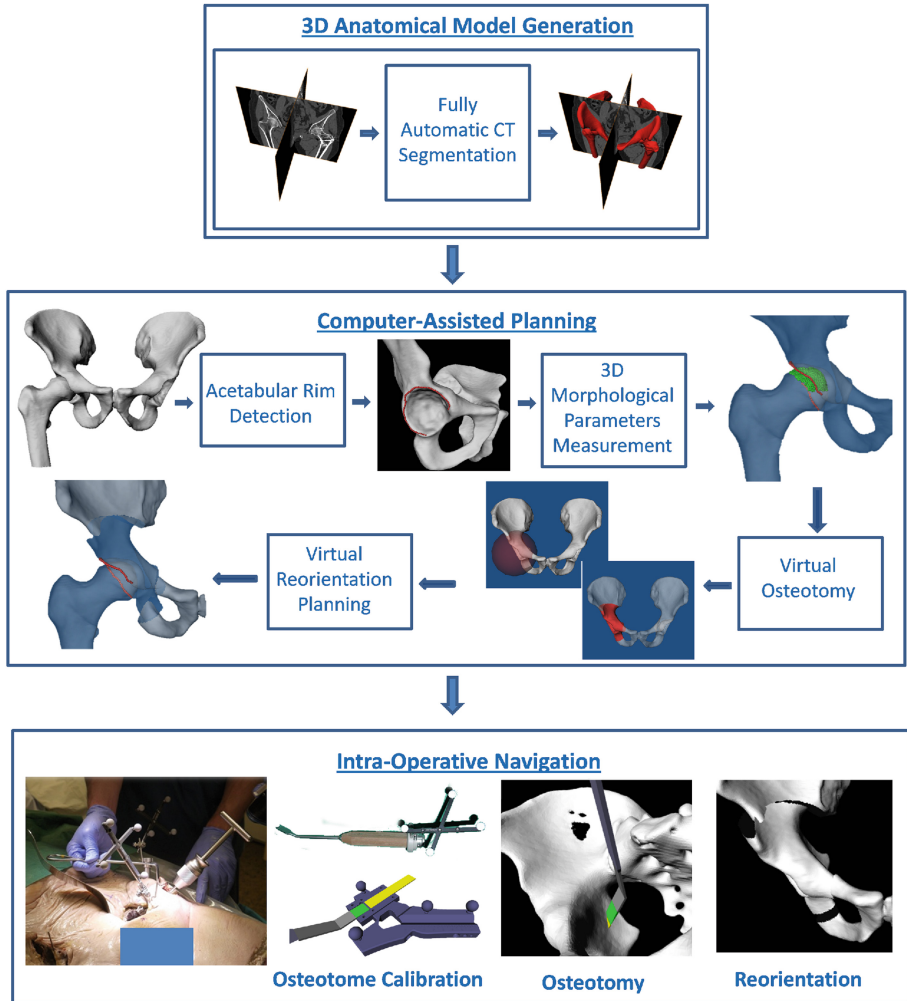


Fig. 1. Schematic view of our computer assisted planning and navigation system for PAO.

2.2 Computer Assisted Diagnosis of Hip Dysplasia

Accurate assessment of acetabular morphology and its relationship to the femoral head is essential for diagnosis of hip dysplasia and PAO planning. After pelvic and femoral surface models are input to our system, the pelvic local coordinate systems is established using anatomical landmarks extracted from the CT data which is defined on the anterior pelvic plane (APP) using the bilateral anterior superior iliac spines (ASISs) and the bilateral pubic tubercles [12]. After local coordinate system is established, a fully automatic detection of the acetabular rim is conducted [11] (see Fig. 2(A)). As soon as acetabular rim points

are extracted, least-squares fitting is used to fit a plane to these points (see Fig. 2(B)). The normal of the fitted plane is defined as the orientation of acetabulum \vec{n}_{CT} . The fitted plane then allows for computing acetabular inclination and anteversion [13] (see Fig. 2(C) and (D)). Additional hip morphological parameters such as the 3D LCE angle, the 3D femoral head EI, the FHC, the anterior coverage of femoral head (AC) and posterior coverage of femoral head (PC) are computed as well (see Fig. 2(E)–(I)). LCE is depicted as an angle formed by a line parallel to the longitudinal pelvic axis defined on the APP and by the line connecting the center of the femoral head with the lateral edge of the acetabulum according to Wiberg [14]. Femoral head EI is defined as the percentage of uncovered femoral head in comparison to the total horizontal head diameter according to Murphy et al. [15]. FHC is defined to be a ratio between the area of the upper femoral head surface covered by the acetabulum and the area of the complete upper femoral head surface from the weight-bearing point of view [16]. The 3D measurements of FHC used in this system is adapted from the method reported in [18]. The difference is that the method [17] that we used now is based on native geometry of the femoral head. In contrast, the work reported in [18] assumed that the femoral head is ideally spherical [18]. In normal hips the assumption is valid since the femoral head is spherical or nearly so. However, in dysplastic hips, the femoral head may be elliptical or deformed [19]. Thus the method [17] used in this system is more accurate than the method that was introduced in [18]. For more details, we refer to [17].

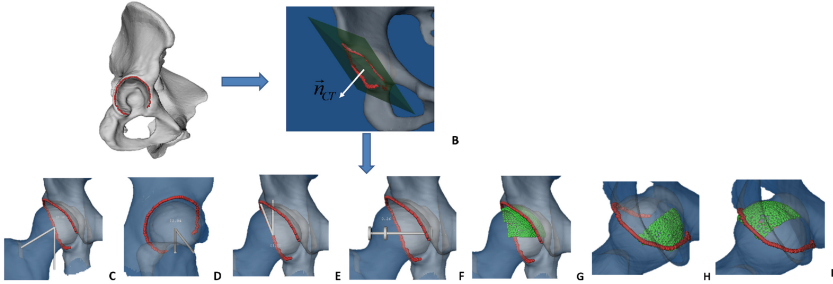


Fig. 2. Computing 3D morphological parameters of the hip joint. (A) Fully automatic acetabular rim detection; (B) Least-squares fitting plane of acetabular rim and the orientation of acetabulum; (C) Acetabular Inclination; (D) Acetabular Anteversion; (E) Lateral Center Edge Angle (LCE); (F) Femoral Head Extrusion Index (EI); (G) Femoral Head Coverage (FHC); (H) Anterior Coverage of Femoral Head (AC); (I) Posterior Coverage of Femoral Head (PC).

2.3 Computer Assisted Planning and Simulation of PAO Treatment

An *in silico* PAO procedure is conducted with our system as follows. First, since the actual osteotomies do not need to be planned as an exact trajectory, a sphere is used to simulate osteotomy operation. More specifically, the center of femoral

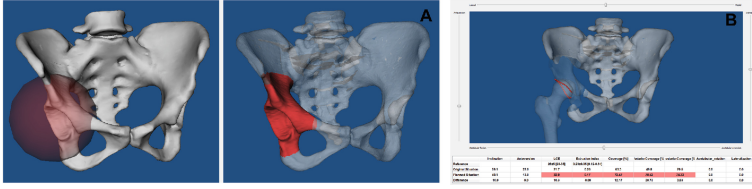


Fig. 3. In silico PAO surgical procedure in our PAO planning system. (A) Virtual osteotomy operation is done with a sphere, whose radius and position can be interactively adjusted; (B) Virtual reorientation operation is done by interactively adjusting anteversion and inclination angle of the acetabulum fragment. The hip morphological parameters (inclination, anteversion, LCE, EI, FHC, AC and PC) are then computed based on the reoriented acetabulum fragment and showed at the bottom of the screen.

head is taken as the center of the sphere whose radius and position can be interactively adjusted along lateral/medial, caudal/cranial, and dorsal/ventral directions, respectively, in order to approximate actual osteotomy operation (see Fig. 3(A)). After that, the in silico PAO procedure is conducted by interactively changing the inclination and the anteversion of the acetabulum fragment (see Fig. 3(B)). During the acetabulum fragment reorientation, 3D LCE angle, EI, FHC, AC and PC are computed in real time based on the reoriented acetabulum fragment and showed at the bottom of the screen (see Fig. 3(B)). Once the morphological parameters of normal hip are achieved (inclination: $45^\circ \pm 4^\circ$, $[37^\circ - 54^\circ]$ [22]; anteversion: $17^\circ \pm 8^\circ$, $[1^\circ - 31^\circ]$ [22]; LCE $> 25^\circ$ [23]; FHC: $73\% \pm 4\%$, $[66\% - 81\%]$ [22]), the planned morphological parameters are stored and subsequently transferred to the navigation module as explained in details in the following section.

2.4 Intra-operative Surgical Navigation

Navigated PAO surgical intervention is described as follow: Before the acetabular fragment is osteotomized, the pelvis is attached with a dynamic reference base (DRB) in order to register the surgical anatomy to the pelvis surface model generated from a pre-operatively acquired CT data (see Fig. 4(A) and (B)). After that, CT-patient registration based on a Restricted Surface Matching (RSM) algorithm [24] is conducted, which is basically divided into two successive steps: a paired point matching followed by a surface matching (see Fig. 4(B)). More specifically, the paired point matching is regarded as an alignment process of pairs of anatomical landmarks. In a pre-operative stage, 4 anatomical landmarks (bilateral ASISs and the bilateral pubic tubercles) are determined on the pelvic model segmented from CT data. In an intra-operative stage, the corresponding landmarks on the patient are digitized using a tracked probe. The digitized points are defined in the coordinate system of the DRB, which is rigidly fixed onto the pelvis. Then the surface matching computes the registration transformation based on 20–30 scattered points around the accessible surgical site that

is matched onto a surface of a pelvic model (see Fig. 4(B)). After registration, the osteotomes are calibrated using a multi-tools calibration unit in order to determine the size and orientation of the blade plane (see Fig. 4(C)). The tip of the osteotome is shown in relation to the virtual bone model, axial, sagittal and coronal views of the actual CT dataset. The cutting trajectory is visualized in real time by prolongation of the blade plane of the osteotome. Thus the osteotomies can be performed in a controlled manner and complications such as intraarticular penetration and accidental transection of the posterior column can be avoided [2] (see Fig. 4(D)). After the acetabular fragment is mobilized from the pelvis, another DRB is anchored to the acetabulum area for intra-operative tracking, thereby the acetabular reorientation can be supported by the navigation module. The navigation system can provide interactive measurements of acetabular morphological parameters and image-guidance information, which instantaneously updates the virtual display, current position and orientation parameters of the acetabulum and the planned situation (inclination and anteversion angles) derived from the pre-operative planning module. The surgeon repositions the acetabulum by controlling its inclination and anteversion angle in order to determine whether the current position achieves the pre-operatively planned position or further adjustment is required (see Fig. 4(E)). After successful repositioning, preliminary K-wire fixation and finally definitive screw fixation is conducted [20]. In this sawbone validation study, a 3D articulated arm (FISSO[®], 3D Articulated Gaging Arms, Switzerland) is employed to anchor the fragment for navigation accuracy evaluation (see Fig. 4(A)).

2.5 Study Design

In order to validate this newly developed planning and navigation system for PAO, two validation studies were designed and conducted on 4 sawbone models. The purpose of the first study is to evaluate the intra-operative accuracy and reliability of navigation system. The second study is designed to evaluate whether the acetabulum repositioning based on navigated PAO procedure can achieve the pre-operative planned situation by comparing the measured acetabular orientation parameters between pre-operative and post-operative CT data.

In the first study, pre-operative planning was conducted with the PAO planning module. Subsequently the intra-operative navigation module was used to track acetabular and pelvic fragments, supporting and guiding the surgeon to adjust the inclination and anteversion angles of acetabulum interactively. Acetabular reorientation measured by the inclination and anteversion angles can be planned pre-operatively and subsequently realized intra-operatively without significant difference. In order to assess the error difference between the pre-operatively planned and the intra-operatively achieved acetabular orientation, we compared the decomposed rotation components derived from the acetabular fragment reorientation between the planned and intra-operative situations.

In the following, all related coordinate systems are first defined before the details about how to compute decomposed rotation components will be presented. Pre-operatively all related coordinate systems are defined (Fig. 5) on the virtual

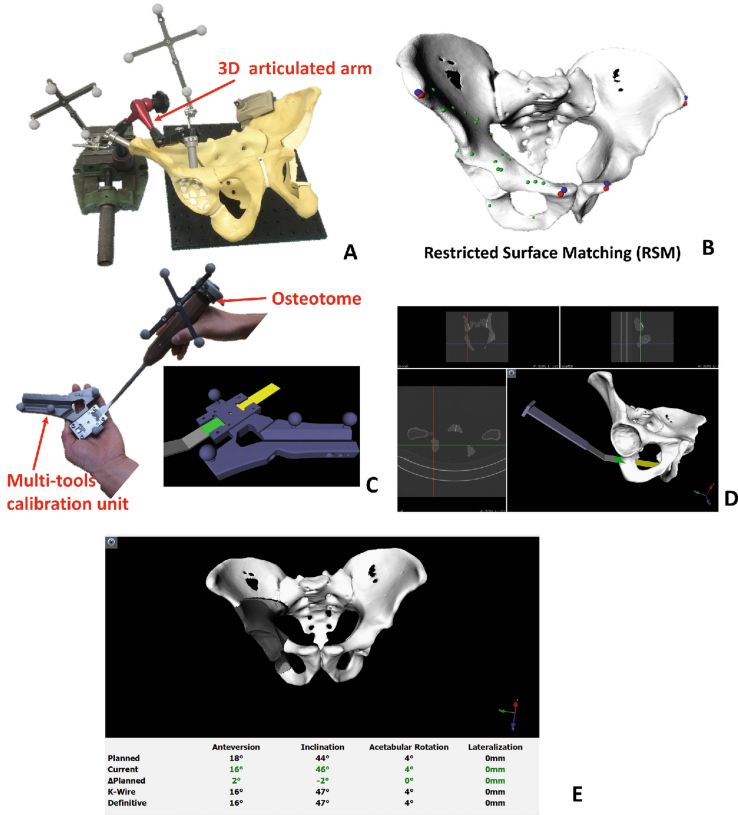


Fig. 4. Intra-operative PAO surgical navigation. (A) Setup of the navigated PAO surgery where two dynamic reference bases (DRBs) with reflective spheres are attached to both the iliac crest and the acetabular fragment; (B) The areas of the pelvis acquired with the tracked probe to perform the RSM registration; (C) Osteotome calibration unit where the green part represents the blade plane of the osteotome and the yellow part represents the prolongation of the blade plane; (D) Screenshot of CT-based osteotomy guidance where the tip of the osteotome is displayed on axial, sagittal and coronal views of the CT dataset, and a cutting trajectory is displayed on the bony model; (E) Screenshot of navigated reorientation procedure. (Color figure online)

3D model with Ref_{CT} representing the pre-operative CT data coordinate system of the surface model. $(Ref_{APP})^{Pre}$ represents the local coordinate system established on the APP, which is defined manually by choosing four landmarks (left and right anterior superior iliac spine [ASIS] and left and right pubic tubercle). Using the acetabular rim points extracted in the Ref_{CT} , acetabular version and inclination can be calculated in relation to $(Ref_{APP})^{Pre}$. Intra-operatively, the Ref_P represents the intra-operative pelvic coordinate system defined on the pelvic DRB, while Ref_A represents the intra-operative acetabulum coordinate system defined on acetabular DRB (Fig. 5(A)). The intra-operative APP coordi-

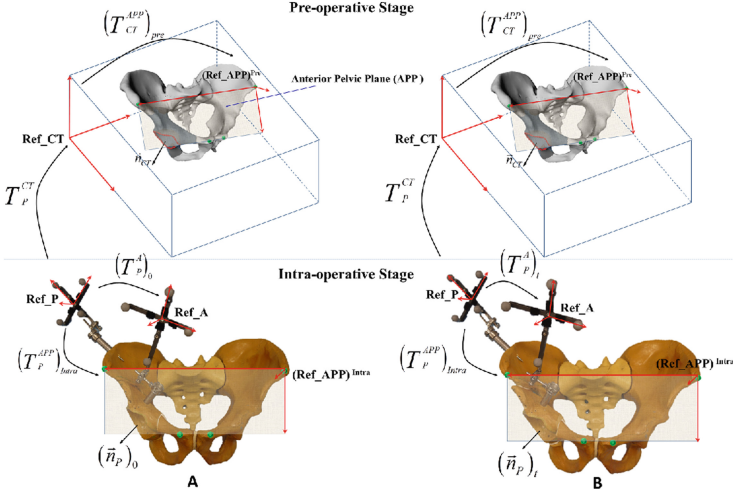


Fig. 5. Precise estimation of acetabular position. (A) Estimation of orientation of acetabulum in the native position before fragment reorientation; (B) Estimation of orientation of acetabulum during fragment reorientation.

nate system is defined by intra-operative paired-point matching [21] of the above-named landmarks and is represented by $(Ref_APP)^{Intra}$. Following the definition of all related coordinate systems, details about how to compute decomposed rotation components are described below.

- **Step 1:** In order to register Ref_CT to Ref_P the DRBs are fixated and a RSM algorithm [24] is performed before the osteotomies and the acetabular fragment tracking. The transformation $(T_P^{APP})_{Intra}$ between the Ref_P and the $(Ref_APP)^{Intra}$ can be calculated by Eq. (1).

$$(T_P^{APP})_{Intra} = (T_{CT}^{APP})_{Pre} \cdot T_P^{CT} \quad (1)$$

where T_P^{CT} is the rigid transformation between the Ref_P and the Ref_CT derived from paired-point matching; $(T_{CT}^{APP})_{Pre}$ is the transformation between the Ref_CT and the $(Ref_APP)^{Pre}$.

- **Step 2:** Before the fragment is moved, a snapshot of the neutral positional relationship between Ref_A and the Ref_P is recorded (Fig. 5(A)). At this moment, the orientation of the acetabulum $(\mathbf{n}_{APP})_{Intra}^0$ with respect to the $(Ref_APP)^{Intra}$ can be estimated by the following equation (Fig. 5):

$$(\mathbf{n}_{APP})_{Intra}^0 = (T_P^{APP})_{Intra} \cdot (\mathbf{n}_P)_0 = (T_P^{APP})_{Intra} \cdot (T_A^P)_0 \cdot (T_P^A)_0 \cdot T_{CT}^P \cdot \mathbf{n}_{CT} \quad (2)$$

where \mathbf{n}_{CT} denotes the orientation of acetabulum measured in the Ref_CT pre-operatively. Equation (2) indicates that one can first compute the

orientation of acetabulum $(\mathbf{n}_P)_0$ with respect to the Ref_P and then transform it to the $(Ref_APP)^{Intra}$ through a transformation train.

- **Step 3:** Fragment mobility is measured by the navigation system, which records the instantaneous positional relationship $(T_A^P)_t$ between the Ref_A and the Ref_P . The neutral positional relationship $(T_A^P)_0$ obtained from **Step 2** is used to calculate the orientation of acetabulum $(\mathbf{n}_P)_t$ with respect to the Ref_P during motion. The instantaneous orientation of acetabulum $(\mathbf{n}_{APP})_{Intra}^t$ with respect to the $(Ref_APP)^{Intra}$ can be calculated by the following equation (Fig. 5(B)):

$$(\mathbf{n}_{APP})_{Intra}^t = (T_P^{APP})_{Intra} \cdot (\mathbf{n}_P)_t = (T_P^{APP})_{Intra} \cdot (T_A^P)_t \cdot (T_P^A)_0 \cdot T_{CT}^P \cdot \mathbf{n}_{CT} \quad (3)$$

Equation (3) indicates that one can first compute the instantaneous orientation of acetabulum $(\mathbf{n}_P)_t$ with respect to the Ref_P and then transform it to the $(Ref_APP)^{Intra}$ through a transformation train.

- **Step 4:** The $(\mathbf{n}_{APP})_{Intra}^0$ and $(\mathbf{n}_{APP})_{Intra}^t$ can then be decomposed into three motion components (Extension/Flexion, External Rotation/Internal Rotation, and Abduction/Adduction) along x-, y- and z axis of the $(Ref_APP)^{Intra}$.

In the second study, we evaluated post-operatively the repositioning of the acetabular fragment and compared this with the pre-operative planned acetabular orientation parameters. Specifically, the acetabular rim points after reorientation were digitized with a tracked probe and transformed to pre-operative CT space based on the aforementioned registration transformation T_{CT}^P . The transformed acetabular rim points was then imported into the computer assisted PAO diagnosis module to quantify acetabular orientation parameters (inclination and anteversion) and compared them with the pre-operatively planned acetabular orientation parameters.

Table 1. The difference ($^\circ$) of decomposed motion components between pre-operative planning and intra-operative navigation situations.

Bones	Side	Flex/Ext	Abd/Add	Ext Rot/Int Rot
#1	Left	0.9	0.1	3.6
#1	Right	0.5	0.5	0.7
#2	Left	0.5	0.4	1.1
#2	Right	0.4	0.1	0.2
#3	Left	0.9	0.1	1.2
#3	Right	0.4	0.5	1.2
#4	Left	0.4	0	0.2
#4	Right	1.0	0.3	0.7
<i>Mean ± STD [Min, max]</i>		<i>0.6 ± 0.3 [0.4, 1.0]</i>	<i>0.3 ± 0.2 [0.0, 0.5]</i>	<i>1.1 ± 1.1 [0.2, 3.6]</i>

3 Results

In the first intra-operative evaluation study, the decomposed rotation components of the acetabular fragment between the pre-operatively planned situation and the intra-operatively achieved situation were compared. According to Table 1, 8 groups of acetabular reorientation data were obtained. It can be seen that the average errors along three motion components (Flexion/Extension, Abduction/Adduction and External Rotation/Internal Rotation) are $0.6^\circ \pm 0.3^\circ$, $0.3^\circ \pm 0.2^\circ$ and $1.1^\circ \pm 1.1^\circ$, respectively.

In the second post-operative evaluation study, the morphological parameters of hip joint between the pre-operatively planned situation and post-operatively repositioned situation were compared. The results are shown in Table 2. From this table, it can be seen that the average errors of acetabular orientation parameters (inclination and anteversion angles) are $0.9^\circ \pm 0.3^\circ$ and $0.9^\circ \pm 0.7^\circ$, respectively. The results are accurate enough from a clinical point of view for PAO surgical intervention and verify the hypothesis that the pre-operatively planned situation can be achieved by navigated PAO procedure with reasonable accuracy.

Table 2. The error of hip joint morphological parameters (IN: Inclination; AV: Anteversion) between pre-operative planning and post-operative evaluation.

Parameter	Stage	#1	#2	#3	#4	#5	#6	#7	#8	Average error
IN ($^\circ$)	Pre-op	41.4	44.2	44.2	42.6	41.9	40.8	50.4	44.6	0.9 ± 0.3 [0.4, 1.2]
IN ($^\circ$)	Post-op	42.6	45.3	44.6	43.8	41.1	40.0	49.3	45.3	
AV ($^\circ$)	Pre-op	13.2	15.1	8.1	8.6	15.3	8.5	10.2	10.3	0.9 ± 0.7 [0.0, 1.7]
AV ($^\circ$)	Post-op	15.2	16.1	9.6	6.9	15.9	8.5	10.5	10.6	

4 Discussions and Conclusions

In this paper, we presented a comprehensive planning, simulation and navigation system for PAO, and evaluated system efficacy with a sawbone study. Previously, the intra-operative accuracy of the navigation system has been also assessed in a cadaver study in order to investigate the technical feasibility of the pararectus surgical approach [25]. As demonstrated by the results in both sawbone and cadaver studies, the efficacy of navigation system is validated with a reasonable accuracy. Based on the results, we are applying ethics approval for a clinical trial where the efficacy of our system will be further evaluated.

References

1. Murphy, S.B., Millis, M.B., Hall, J.E.: Surgical correction of acetabular dysplasia in the adult: a Boston experience. *Clin. Orthop. Relat. Res.* **363**, 38–44 (1999)
2. Ganz, R., Klaue, K., Vinh, T.S., Mast, J.W.: A new periacetabular osteotomy for the treatment of hip dysplasias technique and preliminary results. *Clin. Orthop. Relat. Res.* **232**, 26–36 (1988)

3. Hipp, J.A., Sugano, N., Millis, M.B., Murphy, S.B.: Planning acetabular redirection osteotomies based on joint contact pressures. *Clin. Orthop. Relat. Res.* **364**, 134–143 (1999)
4. Myers, S., Eijer, H., Ganz, R.: Anterior femoroacetabular impingement after periacetabular osteotomy. *Clin. Orthop. Relat. Res.* **363**, 93–99 (1999)
5. Ziebarth, K., Balakumar, J., et al.: Bernese periacetabular osteotomy in males: is there an increased risk of femoroacetabular impingement (FAI) after bernese periacetabular osteotomy? *Clin. Orthop. Relat. Res.* **469**(2), 447–453 (2011)
6. Crockarell Jr., J., Trousdale, R.T., Cabanela, M.E., Berry, D.J.: Early experience and results with the periacetabular osteotomy: the Mayo clinic experience. *Clin. Orthop. Relat. Res.* **363**, 45–53 (1999)
7. Abraham, C., Rodriguez, J., Buckley, J., Burch, S., Diab, M.: An evaluation of the accuracy of computer assisted surgery in preoperatively three dimensionally planned periacetabular osteotomies. In: *ASME 2009 Summer Bioengineering Conference*, pp. 255–256 (2009)
8. Hsieh, P.H., Chang, Y.H., Shih, C.H.: Image-guided periacetabular osteotomy: computer-assisted navigation compared with the conventional technique: a randomized study of 36 patients followed for 2 years. *Acta Orthop.* **77**(4), 591–597 (2006)
9. Langlotz, F., Bächler, R., Berlemann, U., Nolte, L.P., Ganz, R.: Computer assistance for pelvic osteotomies. *Clin. Orthop. Relat. Res.* **354**, 92–102 (1998)
10. Murphy, R.J., Armiger, R.S., Lepistö, J., Mears, S.C., Taylor, R.H., Armand, M.: Development of a biomechanical guidance system for periacetabular osteotomy. *Int. J. Comput. Assist. Radiol. Surg.* **10**(4), 497–508 (2014)
11. Chu, C., Bai, J., Wu, X., Zheng, G.: MASCG: multi-atlas segmentation constrained graph method for accurate segmentation of hip CT images. *Med. Image Anal.* **26**(1), 173–184 (2015)
12. Zheng, G., Marx, A., et al.: A hybrid CT-free navigation system for total hip arthroplasty. *Comput. Aided Surg.* **7**(3), 129–145 (2002)
13. Murray, D.: The definition and measurement of acetabular orientation. *J. Bone Joint Surg. (Br.)* **75**(2), 228–232 (1993)
14. Wiberg, G.: The anatomy and roentgenographic appearance of a normal hip joint. *Acta Chir. Scand.* **83**(Suppl. 58), 7–38 (1939)
15. Murphy, S.B., Ganz, R., Müller, M.: The prognosis in untreated dysplasia of the hip. A study of radiographic factors that predict the outcome. *J. Bone Joint Surg.* **77**(7), 985–989 (1995)
16. Konishi, N., Mieno, T.: Determination of acetabular coverage of the femoral head with use of a single anteroposterior radiograph. A new computerized technique. *J. Bone Joint Surg.* **75**(9), 1318–1333 (1993)
17. Cheng, H., Liu, L., Yu, W., Zhang, H., Luo, D., Zheng, G.: Comparison of 2.5D and 3D quantification of femoral head coverage in normal control subjects and patients with hip dysplasia. *PLoS ONE* **10**(11), e0143498 (2015)
18. Liu, L., Ecker, T., Schumann, S., Siebenrock, K., Nolte, L., Zheng, G.: Computer assisted planning and navigation of periacetabular osteotomy with range of motion optimization. In: *Golland, P., Hata, N., Barillot, C., Hornegger, J., Howe, R. (eds.) MICCAI 2014, Part II. LNCS, vol. 8674, pp. 643–650. Springer, Heidelberg (2014)*
19. Steppacher, S.D., Tannast, M., Werlen, S., Siebenrock, K.: Femoral morphology differs between deficient and excessive acetabular coverage. *Clin. Orthop. Relat. Res.* **466**(4), 782–790 (2008)
20. Olson, S.A.: The bernese periacetabular osteotomy: a review of surgical technique. *Duke Orthop. J.* **1**(1), 21–26 (2010)

21. Lavallee, S.: Registration for computer-integrated surgery: methodology. In: *Computer-Integrated Surgery: Technology and Clinical Applications*, p. 77 (1996)
22. Dandachli, W., Kannan, V., Richards, R., Shah, Z., Hall-Craggs, M., Witt, J.: Analysis of cover of the femoral head in normal and dysplastic hips new CT-based technique. *J. Bone Joint Surg. (Br.)* **90**(11), 1428–1434 (2008)
23. Zou, Z., Chávez-Arreola, A., et al.: Optimization of the position of the acetabulum in a ganz periacetabular osteotomy by finite element analysis. *J. Orthop. Res.* **31**(3), 472–479 (2013)
24. Bächler, R., Bunke, H., Nolte, L.P.: Restricted surface matching numerical optimization and technical evaluation. *Comput. Aided Surg.* **6**(3), 143–152 (2001)
25. Liu, L., Zheng, G., et al.: Periacetabular osteotomy through the pararectus approach: technical feasibility and control of fragment mobility by a validated surgical navigation system in a cadaver experiment. *International Orthopaedics* (2016, in press)



<http://www.springer.com/978-3-319-43774-3>

Medical Imaging and Augmented Reality
7th International Conference, MIAR 2016, Bern,
Switzerland, August 24-26, 2016, Proceedings
Zheng, G.; Liao, H.; Jannin, P.; Cattin, P.C.; Lee, S.-L.
(Eds.)
2016, XVII, 441 p. 202 illus., Softcover
ISBN: 978-3-319-43774-3